Research Square

Preprints are preliminary reports that have not undergone peer review.
They should not be considered conclusive, used to inform clinical practice,
or referenced by the media as validated information.

Cell-specific Associations Between Ferroptosis-related Genes and the Risk of Subarachnoid Hemorrhage: A Mendelian Randomization Study Based on sc-eQTLs from 14 Immune Cell Types

Xiaohan Yang
Qingdao University
Dantong Han
Shandong Medical and Pharmaceutical University
Shaowan Yang
Yuhuangding Hospital
Han Meng
Qingdao University
Xiaodi Chen
Yuhuangding Hospital
Xiao Xiao
Yuhuangding Hospital
Jiajia Yun
The Fourth Affiliated Hospital of Soochow University (Suzhou Dushu Lake Hospital)
Chao Ren
renchaotg@126.com

Yuhuangding Hospital

Research Article

Keywords: Subarachnoid hemorrhage, ferroptosis gene, cofilin-1, immune cells, Mendelian randomization

Posted Date: October 30th, 2026

DOI: https://doi.org/10.21203/rs.3.rs-11190555/v1

License: This work is licensed under a Creative Commons Attribution 4.0 International License.
Read Full License

Additional Declarations: No competing interests reported.

Abstract

Background and Objectives

Subarachnoid hemorrhage (SAH) involves multiple intertwined pathological processes, among which ferroptosis and immune-inflammatory responses are vital. However, the genetic causal effects of ferroptosis-related genes on SAH risk and their immunocellular type specificity remain unclear. This study aimed to investigate the association between ferroptosis-related genes and SAH and its immunocellular type specificity.

Methods

This study integrated expression quantitative trait loci (eQTL) data for ferroptosis-related genes, pooled genome-wide association study data for SAH, Gene Expression Omnibus (GEO) transcriptomic data, and single-cell (sc)-eQTL data. We used Mendelian randomization(MR) analysis to identify genes associated with SAH risk and validated these findings using independent eQTL datasets and GEO differential expression analysis. The inverse-variance-weighted method was used as the primary analytical approach, and sensitivity analyses assessed robustness. Sc-eQTL data were further used to explore immune cell-type-specific associations.

Results

Based on the initial screening using eQTLGen, the genetically predicted expression levels of 48 ferroptosis-related genes were significantly associated with SAH risk. Among them, the elevated *CFL1* gene expression was associated with reduced SAH risk. This result was consistent across genotype-tissue expression whole-blood dataset. Combined with GEO differential expression results, *CFL1* was identified as a key candidate gene. Finally, sc-eQTL analysis revealed that *CFL1* gene expression in CD8NC cells was significantly associated with reduced SAH risk.

Conclusion

CFL1 may be a key ferroptosis gene associated with SAH; its elevated expression in CD8NC cells is associated with a significantly reduced SAH risk, providing new genetic evidence for exploring potential therapeutic targets for SAH.

1 Introduction

Subarachnoid hemorrhage (SAH) is a serious cerebrovascular disease(Hoh et al. 2023). Although it accounts for a relatively low proportion of all stroke types, it is associated with high mortality and disability rates. Recently, advances in interventional treatment techniques have improved short-term survival rates for patients with SAH(Shen et al. 2026). However, several patients still suffer from numerous neurological deficits that severely impair their quality of life(Etminan and Macdonald 2017). Besides the acute damage caused by the hemorrhage itself, secondary brain injury is a major factor

affecting neurological recovery and long-term prognosis in patients with SAH. Previous studies have revealed that secondary brain injury following SAH involves multiple intertwined pathological processes, including oxidative stress, blood-brain barrier disruption, cerebral edema, inflammatory responses, and abnormal activation and immune cell infiltration(Li et al. 2023).

Among the mechanisms mentioned above, ferroptosis has emerged as a hot topic in SAH studies in recent years. Ferroptosis is a regulated form of cell death primarily characterized by accumulating iron-ion-dependent lipid peroxidation. Its pathogenesis is closely associated with iron metabolism disorders, glutathione metabolism abnormalities, lipid peroxidation, and mitochondrial dysfunction(Dixon et al. 2012; Zhang et al. 2023a; Jin et al. 2026). Following SAH, several red blood cells enter the subarachnoid space and gradually lyse, releasing hemoglobin, heme, and free iron ions(Deng et al. 2023). This can further induce reactive oxygen species (ROS) production and enhance lipid peroxidation, thereby promoting ferroptosis(Kang et al. 2024). Previous studies(Gao et al. 2020; Liu et al. 2022) have revealed that key ferroptosis molecules, including glutathione peroxidase 4 (GPX4), solute carrier family 7 member 11 (SLC7A11), and acyl-CoA synthetase long-chain family member 4 (ACSL4), undergo abnormal changes during the brain injury process following SAH(Li et al. 2021). Inhibiting ferroptosis can, to some extent, alleviate neuronal damage, cerebral edema, and neurological dysfunction. These findings suggest that ferroptosis may be a key mechanism underlying secondary brain injury in SAH and provide a new direction to screen potential therapeutic targets for SAH.

Immune and inflammatory responses are also vital for SAH onset and progression. Following SAH, increased blood-brain barrier permeability allows various peripheral immune cells to cross the barrier and enter the central nervous system, further inducing inflammatory responses and exacerbating cerebral edema, neuronal damage, and microcirculatory dysfunction(Duan et al. 2024). Among these immune cells, including T cells, monocytes, and neutrophils, are vital for the progression of inflammation following SAH(Pfnür et al. 2025). Studies have revealed that CD8 + T cells and their cytotoxic subsets can contribute to tissue damage and the amplification of inflammation by releasing perforin, granzyme, and inflammatory cytokines, suggesting that specific immune cell subsets may be vital for brain injury following SAH(Moraes et al. 2015; Roa et al. 2020; Zhang et al. 2023b). Lipid peroxidation products generated during ferroptosis, along with disrupted iron metabolism and oxidative stress, can affect the activation, migration, and effector functions of immune cells(Ma et al. 2021; Shi et al. 2022). Together, infiltrating immune cells can further promote tissue damage and ferroptosis by releasing inflammatory factors, ROS, and cytotoxic molecules. Therefore, in a disease, including SAH, characterized by hemorrhagic injury, iron metabolism abnormalities, and immune-inflammatory activation, exploring the regulatory roles of ferroptosis-related genes in specific immune cells may further elucidate its pathogenesis. Previous animal studies suggest that ferroptosis may contribute to brain injury following SAH by promoting lipid peroxidation, oxidative stress, and inflammatory responses(Gao et al. 2020; Kuang et al. 2021; Li et al. 2021). However, existing evidence primarily comes from *in vitro* studies and animal models; there is still a lack of studies that directly assess the potential causal relationship between the expression of ferroptosis-related genes and susceptibility to SAH at the population genetic level. Mendelian randomization (MR), which uses genetic variation as an instrumental variable, can, to

some extent, reduce the influence of confounding factors and reverse causality in traditional observational studies, thereby providing an effective method for causal inference(Davies et al. 2018). Expression quantitative trait loci (eQTLs) can be used to elucidate the regulatory role of genetic variation on gene expression levels(Võsa et al. 2021).

In contrast, single-cell eQTLs (sc-eQTLs) can further reveal the cell-type specificity of these regulatory effects, thereby providing a basis to identify key cellular subpopulations in which disease-associated genes may play a role. Consequently, this study aimed to integrate eQTL, Gene Expression Omnibus (GEO) differential expression, and sc-eQTL data to systematically screen for key candidate genes involved in ferroptosis that are associated with SAH risk and to further explore their potential cell-type specificity. This study will provide new genetic evidence for the discovery of potential therapeutic targets for SAH and the design of precision intervention strategies.

2 Materials and Methods

2.1 Study Design

This study was designed and reported in accordance with the Strengthening the Reporting of Observational Studies in Epidemiology using Mendelian Randomization (STROBE-MR) guidelines(Skrivankova et al. 2021).We adopted the MR framework to evaluate the potential causal effect of ferroptosis-related gene expression levels on SAH risk and to further explore the cell-type-specific regulatory roles of key genes in immune cells. All data used in this study were derived from publicly available genome-wide association study (GWAS) pooled statistics. We identified single-nucleotide polymorphisms (SNPs) significantly associated with gene expression levels related to exposure variables and used them as instrumental variables (IVs). The selected IVs must satisfy the three core assumptions of MR analysis: (1) Association assumption: Genetic variants serving as instrumental variables must be strongly correlated with the exposure factor. (2) Independence assumption: The genetic variant must not be associated with any confounding factors. (3) Exclusivity constraint: The genetic variant must be influenced only by the exposure.(Davies et al. 2018) The study workflow is presented in **Fig. 1**.

2.2 Data Sources

2.2.1 Gene Data Sources

Data on ferroptosis-related genes were obtained from the FerrDb database (Zhou and Bao 2020)(FerrDb: A manually curated resource for regulators and markers of ferroptosis and ferroptosis-disease associations, https://www.zhounan.org/ferrdb/current/), which is a manually curated database of ferroptosis regulators, markers, and ferroptosis-disease associations.

eQTL data were sourced from the eQTLGen Consortium (https://eqtlgen.org/) and Genotype-Tissue Expression (GTEx, https://www.gtexportal.org/home/).

The eQTLGen dataset comprises blood samples from predominantly healthy European individuals. It evaluates associations between > 11 million variants and the expression levels of 16,989 genes across 31,684 participants from 37 cohorts and 3 gene expression platforms to identify variants associated with whole-blood gene expression (that is, eQTLs). A complete description of the data is provided in the original article(Võsa et al. 2021).

The GTEx database contains 17,382 tissue samples from nearly 1,000 deceased healthy donors(2020). Covering samples from 54 tissue types, the project systematically evaluated the associations between > 13 million variants and the expression levels of approximately 20,000 protein-coding genes. This study focused on data from this database associated with whole blood (Whole_Blood.v10.eQTLs) to further validate the positive genes identified by eQTLGen.

2.2.2 Immune Cell Data

The immune cell data are derived from a large-scale single-cell RNA sequencing study. This study revealed cell-type-specific genetic characteristics of immune system regulation by examining the association between genetic variants and gene expression across 14 immune cell types. It involves 759,993 common genetic variants and their effects on gene expression across 14 immune cell types; specific data are available in the original article(Yazar et al. 2022). This dataset includes 14 distinct immune cell phenotypes, grouped into four major categories: CD4 + T cells (3 phenotypes: CD4 ET, CD4 NC, and CD4 SOX4), CD8 + T cells (3 phenotypes: CD8 ET, CD8 NC, and CD8 S100B), B cells (3 phenotypes: B Mem, B IN, and plasma), natural killer (NK) cells (2 phenotypes: NK and NK R), monocytes (2 phenotypes: Mono C, and Mono NC), and dendritic cells (1 phenotype: DC).

2.2.3 SAH Data

The pooled GWAS statistics for SAH were obtained from the FinnGen database, release 12 (FinnGen R12). FinnGen is a large-scale population-based genetic research project that uses Finnish biobanks to construct disease phenotypes by integrating genotype data with Finland's national health registries(Kurki et al. 2023). FinnGen R12 includes 500,348 participants, covering 2,502 health outcomes and approximately 21.31 million genetic variant loci.

The SAH outcome phenotype selected for this study was coded as I9_SAH. This phenotype is primarily defined based on hospital discharge diagnoses and cause-of-death records from the Finnish National Health Registry, comprising 4,180 cases and 450,276 controls, for 454,456 Finnish records. This aggregated dataset provides information on the genetic association between SNPs and SAH risk, including effect alleles, non-effect alleles, effect sizes, standard errors, *P*-values, and allele frequencies, which can be used for subsequent two-sample MR analyses. Further details regarding the results can be identified at (https://storage.googleapis.com/finngen-public-data-r12/summary_stats/release/finngen_R12_I9_SAH.gz).

2.3 Screening of Candidate Genes Associated with Ferroptosis

We cross-referenced the 15,695 genes obtained from the eQTLGen Consortium with the 483 ferroptosis-associated genes from the FerrDb database(Zhou et al. 2023). A Venn diagram of the results revealed 315 common genes.

2.4 Screening Instrumental Variables Using SNPs

Given that cis-eQTLs are typically located in the vicinity of the target gene and can directly reflect the regulatory effects of genetic variation on the expression levels of neighboring genes, cis-eQTLs exhibit higher instrumental variable specificity and reliability compared to trans-eQTLs, which may involve more complex regulatory relationships(Grover et al. 2017; 2020). Accordingly, this study used cis-eQTLs as genetic instrumental variables for gene expression. To satisfy the correlation assumption of the MR analysis, this study first screened the eQTLGen Consortium dataset for cis-eQTL SNPs significantly associated with the expression levels of genes related to ferroptosis, using $P < 5 \times 10^{-8}$ as the significance threshold(Pavlides et al. 2016). Subsequently, the clump_data function was used to cluster the selected SNPs based on linkage disequilibrium (LD), setting $r^2 < 0.1$ in a 10,000-kb window to remove SNPs with strong LD within the same exposure factor and retain the independent SNP most significantly associated with the exposure as a candidate instrumental variable(Boehm and Zhou 2022; Paz et al. 2023). To avoid weak instrumental variable bias, this study further calculated the F-statistic for each SNP and retained only those with an F-value > 10 as final instrumental variables(Burgess and Thompson 2011). Subsequently, the $harmonize_data$ function was used to harmonize allele information between exposure data and SAH outcome data, and the Steiger directionality test was applied to exclude SNPs where the outcome might reverse-affect the exposure, thereby reducing the risk of violating the exclusivity assumption of MR(Hemani et al. 2017).

To further validate the stability of eQTLGen preliminary screening results, we extracted instrumental variables corresponding to eQTLGen-positive genes from the GTEx dataset. We applied the same screening criteria: $P < 5 \times 10^{-8}$, LD clumping $r^2 < 0.1$, a window size of 10,000 kb, and F > 10. The Wald ratio method was used to estimate MR effects for genes containing only a single instrumental variable. The inverse-variance-weighted (IVW) method was used as the primary analysis method for genes containing multiple instrumental variables(Hartley et al. 2022).

In the sc-eQTL analysis, due to the relatively limited availability of *CFL1* gene-related instrumental variables across different immune cell subtypes, this study adopted a relatively lenient instrumental variable screening threshold of, specifically $P < 0.05$, and set $r^2 < 0.03$ for LD clumping to filter for specific instrumental variables of the *CFL1* gene in 14 immune cell subtypes *(*Hu et al. 2024). Subsequently, the F-statistic for each SNP was calculated, with F > 10 used as the reference standard for the strength of the instrumental variable. (**Supplementary Tables S1–S3)**

2.5 MR Analysis

This study used the IVW method and the Wald ratio (WR) as the primary analytical methods. When an exposure included only one valid instrumental variable, the WR method was used for analysis; that is, the

effect estimate was calculated as the ratio of the effect of that genetic variant on the outcome to its effect on the exposure(Burgess et al. 2013). When two or more mutually independent instrumental variables were included, the IVW method was used for analysis. The IVW method combines the effect estimates by weighting them following the variance of each instrumental variable's effect estimate. Under the assumption that all instrumental variables are valid and there is no directional horizontal multivariate heterogeneity, this method yields a pooled effect estimate with high statistical power(Burgess et al. 2013). To verify the robustness of the main results, supplementary analyses were conducted using the weighted median (WM) method(Bowden et al. 2016), MR-Egger regression(Bowden et al. 2015), weighted mode method, and simple mode method(Hartwig et al. 2017). The WM method draws inferences by calculating the WM of the estimated effects for each instrumental variable; even when only 50% of the total weight comes from valid instrumental variables, relatively reliable estimates can still be obtained. Conversely, the intercept term in MR-Egger regression is primarily used to test for directional horizontal multieffectivity in the instrumental variables. A significant deviation of the intercept term from 0 suggests that genetic variation may influence the outcome through pathways other than the exposure factor. Under the assumption that the strength of the instrumental variables is independent of the direct effect, the slope from MR-Egger regression can provide an adjusted effect estimate even in the presence of horizontal multieffectivity. The weighted mode method selects the effect value with the largest weight; this method is valid only if the group of instrumental variables with the largest weight proportion consists of valid instrumental variables. The simple mode method also directly selects the effect value with the highest frequency; however, it does not assign different weights to the various instrumental variables during the calculation.

2.6 Sensitivity Analysis

To further test the robustness of the MR results, this study conducted several sensitivity analyses. Cochran's Q test was used to assess heterogeneity among the effect estimates of different instrumental variables(Bowden et al. 2017). The MR-Egger intercept test was used to evaluate directional multieffectivity(Bowden et al. 2015), and the MR-PRESSO global test was used to detect potential overall multieffectivity. When the global test indicated the presence of horizontal polypleiotropy, the MR-PRESSO outlier test was used to identify anomalous SNPs, and the overall effect was re-estimated after excluding these outliers(Verbanck et al. 2018). Additionally, a leave-one-out analysis was conducted to determine whether MR results were unduly influenced by a single SNP(Burgess et al. 2019), and funnel plots were used to visually assess the robustness of the results(Bowden et al. 2015).

2.7 Statistical Analysis

All statistical analyses were performed using standard packages in the R software (version 4.5.2), specifically TwoSampleMR (version 0.6.24), MR-PRESSO (version 1.0), foreach (version 1.5.2), ggplot2 (version 4.0.2), forestploter (version 1.1.4), grid (version 4.5.2), and limma (version 3.66.0).

3 Results

3.1 Assessment of the Overall Impact of Expression Levels of Ferroptosis-related Genes on SAH

Following initial screening with eQTLGen, IVW results revealed that the genetically predicted expression levels of 48 ferroptosis-related genes were significantly genetically associated with SAH risk (**Supplementary Table 4**). Given the numerous results, the main text focuses on the eight genes that were subsequently validated in the GTEx whole blood dataset. Elevated *ECH1* gene expression was significantly associated with an increased SAH risk (odds ratio [OR] = 1.1854, 95% confidence interval [CI] = 1.0389–1.3526, *P* = 0.0115). Elevated *ATG7* gene expression was significantly associated with an increased risk of SAH (OR = 1.3120, 95% CI = 1.1500–1.4968, *P* = 0.0001). Elevated *CHP1* gene expression was significantly associated with a reduced risk of SAH (OR = 0.7390, 95% CI = 0.6139–0.8895, *P* = 0.0014). Elevated *RPL8* gene expression was significantly associated with a reduced SAH risk (OR = 0.9452, 95% CI = 0.8962–0.9968, *P* = 0.0378). Elevated *MAP3K11* gene expression was significantly associated with an increased SAH risk (OR = 1.1223, 95% CI = 1.0595–1.1888, *P* = 0.001). Elevated *CFL1* gene expression was significantly associated with a reduced SAH risk (OR = 0.8673, 95% CI = 0.7827–0.9609, *P* = 0.0065). Elevated *GDF15* gene expression was significantly associated with an increased SAH risk (OR = 1.3229, 95% CI = 1.1316–1.5467, *P* = 0.0004). Elevated *MFN2* gene expression was significantly associated with an increased risk of SAH (OR = 1.0405, 95% CI = 1.0041–1.0783, *P* = 0.0291)

Validation using the GTEx database revealed that the genetically predicted expression levels of eight ferroptosis-related genes were significantly associated with SAH risk (**Supplementary Table 5**). For genes with a single SNP, WR results revealed that elevated *ECH1* gene expression was significantly associated with an increased SAH risk (OR = 1.8385, 95% CI = 1.2804–2.6397, *P* = 0.0010); elevated *ATG7* gene expression was significantly associated with an increased SAH risk (OR = 1.8688, 95% CI = 1.2462–2.8025, *P* = 0.0025). Elevated *CHP1* gene expression was significantly associated with a reduced SAH risk (OR = 0.5376, 95% CI = 0.3567–0.8101, *P* = 0.0030). Elevated *CFL1* gene expression was significantly associated with a reduced SAH risk (OR = 0.4341, 95% CI = 0.2002–0.9413, *P* = 0.0346). For genes with multiple SNPs, IVW results revealed that elevated *RPL8* gene expression was significantly associated with reduced SAH risk (OR = 0.7975, 95% CI = 0.6811–0.9339, *P* = 0.0050). Elevated *MAP3K11* gene expression levels were significantly associated with an increased SAH risk (OR = 1.3494, 95% CI = 1.0470–1.7392, *P* = 0.0206). Elevated *GDF15* gene expression levels were significantly associated with an increased SAH risk (OR = 1.1528, 95% CI = 1.0063–1.3205, *P* = 0.0403). Elevated *MFN2* gene expression levels were significantly associated with an increased SAH risk (OR = 1.0706, 95% CI = 1.0025–1.1433, *P* = 0.0420). The main MR effect estimates for the eight genes listed above across different datasets are presented in Table 1.

Table 1
Mendelian randomization results for ferroptosis-related genes associated with subarachnoid hemorrhage in both the eQTLGen and GTEx whole blood datasets

Gene	eQTL dataset	nSNP	Method	Beta	SE	OR (95% CI)	*P* value
ECH1	eQTLGen	11	IVW	0.1701	0.0673	1.1854 (1.0389–1.3526)	0.0115
	GTEx	1	Wald ratio	0.6089	0.1846	1.8385 (1.2804–2.6397)	0.0010
ATG7	eQTLGen	18	IVW	0.2715	0.0672	1.3120 (1.1500–1.4968)	0.0001
	GTEx	1	Wald ratio	0.6253	0.2067	1.8688 (1.2462–2.8025)	0.0025
CHP1	eQTLGen	9	IVW	-0.3025	0.0946	0.7390 (0.6139–0.8895)	0.0014
	GTEx	1	Wald ratio	-0.6207	0.2092	0.5376 (0.3567–0.8101)	0.0030
RPL8	eQTLGen	46	IVW	-0.0564	0.0271	0.9452 (0.8962–0.9968)	0.0378
	GTEx	9	IVW	-0.2262	0.0805	0.7975 (0.6811–0.9339)	0.0050
MAP3K11	eQTLGen	53	IVW	0.1154	0.0294	1.1223 (1.0595–1.1888)	0.0001
	GTEx	2	IVW	0.2997	0.1295	1.3494 (1.0470–1.7392)	0.0206
CFL1	eQTLGen	13	IVW	-0.1424	0.0523	0.8673 (0.7827–0.9609)	0.0065

Only the primary MR estimate for each gene in each dataset is presented. For exposures with one instrumental variable, the Wald ratio method was used; for exposures with two or more instrumental variables, the inverse-variance weighted method was used. Beta represents the log odds ratio of SAH per genetically predicted increase in gene expression. eQTL, expression quantitative trait locus; GTEx, Genotype-Tissue Expression; IVW, inverse-variance weighted; MR, Mendelian randomization; nSNP, number of single-nucleotide polymorphisms; OR, odds ratio; CI, confidence interval; SE, standard error; SAH, subarachnoid hemorrhage.

Gene	eQTL dataset	nSNP	Method	Beta	SE	OR (95% CI)	*P* value
	GTEx	1	Wald ratio	-0.8345	0.3949	0.4341 (0.2002–0.9413)	0.0346
GDF15	eQTLGen	8	IVW	0.2799	0.0797	1.3229 (1.1316–1.5467)	0.0004
	GTEx	2	IVW	0.1422	0.0693	1.1528 (1.0063–1.3205)	0.0403
MFN2	eQTLGen	53	IVW	0.0397	0.0182	1.0405 (1.0041–1.0783)	0.0291
	GTEx	4	IVW	0.0682	0.0335	1.0706 (1.0025–1.1433)	0.0420

Only the primary MR estimate for each gene in each dataset is presented. For exposures with one instrumental variable, the Wald ratio method was used; for exposures with two or more instrumental variables, the inverse-variance weighted method was used. Beta represents the log odds ratio of SAH per genetically predicted increase in gene expression. eQTL, expression quantitative trait locus; GTEx, Genotype-Tissue Expression; IVW, inverse-variance weighted; MR, Mendelian randomization; nSNP, number of single-nucleotide polymorphisms; OR, odds ratio; CI, confidence interval; SE, standard error; SAH, subarachnoid hemorrhage.

To further illustrate the overall distribution of MR effect estimates and statistical significance for ferroptosis-related genes, we generated volcano plots based on eQTLGen and GTEx whole-blood data. Preliminary screening results from eQTLGen revealed that the genetically predicted expression levels of 48 ferroptosis-related genes were significantly associated with SAH risk. Among these, *ECH1, ATG7, CHP1, RPL8, MAP3K11, CFL1, GDF15*, and *MFN2*, which were subsequently validated in the GTEx dataset, are highlighted in the Figure. In GTEx validation results, all eight genes reached statistical significance. Notably, for *CFL1*, the direction of effect indicated that higher genetically predicted expression was associated with a reduced risk of SAH. This gene was subsequently identified as a key candidate gene in a GEO differential expression cross-screening analysis (**Fig. 2**).

3.2 Cross-validation of Differentially Expressed Genes and Key Candidate Genes Associated with SAH

To further validate the candidate genes identified through MR analysis at the transcriptomic level, we retrieved sequence matrix data from the GEO database using the keyword “Subarachnoid Hemorrhage.” We set the following specific search criteria: “Study Type” was set to “Expression profiling by array,” and the species was limited to humans. The data included peripheral blood samples from patients with diseases closely associated with SAH (GSE13353), annotated as GPL570. Subsequently, gene IDs were

converted to gene symbols based on the platform annotation file to facilitate data analysis and interpretation. Ultimately, 1,358 differentially expressed genes were identified.

We cross-referenced the genes identified in the initial screening and validation with those associated with the disease. This analysis identified an overlapping gene, *CFL1*. In the eQTLGen database, genetically predicted upregulation of *CFL1* expression was significantly associated with a reduced risk of SAH (OR = 0.8673, 95% CI = 0.7827–0.9609, *P* = 0.0065). Validation using GTEx whole-blood eQTL data confirmed this trend (OR = 0.4341, 95% CI = 0.2002–0.9413, *P* = 0.0346), further supporting a potential causal association between *CFL1* and SAH risk.

3.3 Evaluation of Cell-type-specific Effects of the Expression of the Key Candidate Gene CFL1 in Immune Cell Subtypes on SAH

We conducted MR analysis of the genetically predicted expression levels of *CFL1* in different immune cell subtypes based on sc-eQTL data. Raw sc-eQTL data covered 14 immune cell subtypes. Among them, genetic variants suitable for MR analysis were identified in 11 subtypes following instrumental variable screening. The main MR results for each cell subtype are listed in Table 2. Using the IVW method as the primary analysis approach, the results revealed that higher genetically predicted *CFL1* expression in CD8NC cells was significantly associated with a reduced risk of SAH (OR = 0.7500, 95% CI = 0.5955–0.9446, *P* = 0.0145). The results from the WM method were consistent in direction, suggesting that elevated *CFL1* expression was associated with a reduced SAH risk (OR = 0.7227, 95% CI = 0.5306–0.9842, *P* = 0.0393). In other immune cell subtypes, no consistent significant association was observed between *CFL1* gene expression levels and SAH risk. The detailed results are presented in **Supplementary Table 6**.

Table 2
Mendelian randomization estimates for the association between genetically predicted CFL1 expression in eligible immune cell subtypes and subarachnoid hemorrhage

Cell ID	Immune cell subtype	nSNP	Method	Beta	SE	OR (95% CI)	*P* value
bmem	Memory B cell	1	Wald ratio	-0.0786	0.4074	0.9245 (0.4160–2.0544)	0.8471
cd4et	CD4 effector memory/TEMRA	3	Inverse variance weighted	-0.1051	0.1981	0.9002 (0.6105–1.3273)	0.5956
cd4nc	CD4 naive/central memory T cell	4	Inverse variance weighted	-0.1936	0.1238	0.8240 (0.6465–1.0502)	0.1178
cd4sox4	CD4 SOX4 T cell	1	Wald ratio	0.2179	0.2037	1.2434 (0.8341–1.8536)	0.2848
cd8et	CD8 effector memory T cell	1	Wald ratio	-0.3743	0.3675	0.6878 (0.3346–1.4135)	0.3085
cd8nc	CD8 naive/central memory T cell	4	Inverse variance weighted	-0.2877	0.1177	0.7500 (0.5955–0.9446)	0.0145*
cd8s100b	CD8 S100B T cell	1	Wald ratio	-0.1180	0.2098	0.8887 (0.5891–1.3407)	0.5737
dc	Dendritic cell	4	Inverse variance weighted	-0.0773	0.1776	0.9257 (0.6535–1.3112)	0.6636
monoc	Classical monocyte	2	Inverse variance weighted	0.0109	0.1984	1.0109 (0.6852–1.4915)	0.9563
nk	Natural killer cell	3	Inverse variance weighted	-0.0425	0.1219	0.9584 (0.7546–1.2172)	0.7275
plasma	Plasma cell	2	Inverse variance weighted	0.1562	0.4500	1.1691 (0.4840–2.8239)	0.7284

The source single-cell eQTL dataset comprised 14 immune cell types; 11 cell subtypes had at least one eligible CFL1 instrumental variable after instrument selection and were included in the MR analysis. The principal estimate is shown for each cell subtype: Wald ratio for one SNP and IVW for two or more SNPs. CFL1, cofilin-1; eQTL, expression quantitative trait locus; IVW, inverse-variance weighted; MR, Mendelian randomization; OR, odds ratio; CI, confidence interval; SE, standard error; SNP, single-nucleotide polymorphism; SAH, subarachnoid hemorrhage. *$P < 0.05$.

3.4 Sensitivity Analysis Results

To ensure the reliability of the above associations, this study conducted systematic sensitivity tests: (1) The MR-Egger intercept analysis did not reveal significant horizontal polypleiotropy bias ($P > 0.05$); (2) the MR-PRESSO global test confirmed the absence of anomalous polypleiotropy ($P > 0.05$); (3) Cochran's Q test revealed non-significant heterogeneity among SNPs ($P > 0.05$) (Supplementary Tables S7–9). To assess the robustness of the primary MR results for *CFL1*, this study further performed heterogeneity and horizontal polygenic bias tests on multi-instrumental variable analyses in eQTLGen, GTEx, and CD8NC cell sc-eQTL datasets. The results are presented in Table 3. MR analysis results based on the eQTLGen database revealed that there was non-significant heterogeneity among the instrumental variables for *CFL1* (Cochran's Q = 6.5022, $P = 0.8887$), and the MR-Egger intercept test did not detect significant horizontal polygenic effects (Egger intercept = − 0.0037, $P = 0.8353$), suggesting that there was non-significant heterogeneity or horizontal pleiotropy among the genetic instrumental variables. Furthermore, in the GTEx database validation, non-significant heterogeneity or pleiotropy was observed for *CFL1* (since *CFL1* contains only a single instrumental variable, Cochran's Q and the MR-Egger intercept test could not be performed). In the immune cell-specific MR analysis based on sceQTL data, the genetic instrumental variable for *CFL1* in CD8NC cells also revealed non-significant heterogeneity (Cochran's Q = 2.7905, $P = 0.4251$), and the MR-Egger intercept test did not indicate horizontal polyvalence (Egger intercept = 0.1097, $P = 0.6817$). These results indicate that the genetic association between *CFL1* and SAH risk identified in this study is robust. Furthermore, scatter, funnel, forest, and leave-one-out sensitivity analysis plots **(Figs. 3–7**) visually confirm the high robustness of the results.

Table 3
Sensitivity analyses of the associations between genetically predicted CFL1 expression and subarachnoid hemorrhage

Data source / cell type	nSNP	Primary method	Cochran's Q	Q-*P* value	MR-Egger intercept	*P* value
eQTLGen	13	IVW	6.5022	0.8887	−0.0037	0.8353
GTEx	1	Wald ratio	NA	NA	NA	NA
sc-eQTL CD8NC	4	IVW	2.7905	0.4251	0.1097	0.6817

Cochran's Q test was used to assess heterogeneity, and the MR-Egger intercept test was used to evaluate directional horizontal pleiotropy. Because CFL1 was instrumented by only one SNP in the GTEx whole-blood dataset, heterogeneity and MR-Egger intercept tests were not applicable. CFL1, cofilin-1; SAH, subarachnoid hemorrhage; IVW, inverse-variance weighted; sc-eQTL, single-cell expression quantitative trait locus; CD8NC, CD8 natural killer-like cytotoxic cells; SNP, single-nucleotide polymorphism; NA, not applicable.

4 Discussion

4.1 *CFL1* Gene Expression and Its Role in Cell-specific Immune Regulation in CD8NC Cells

This study found that elevated genetically predicted expression of the ferroptosis-related gene *CFL1* in CD8NC cells was significantly associated with reduced SAH risk. Cofilin-1, encoded by the *CFL1* gene, is an important member of the ADF/cofilin family and is widely expressed in mammals(Samstag et al. 2013). Cofilin-1 binds to G-actin and F-actin and promotes the renewal of the actin network by cleaving and depolymerizing actin filaments to generate new actin ends(Hayden et al. 1993). Besides its classic role in cytoskeletal regulation, cofilin-1 possesses redox sensitivity and mitochondrial regulatory functions(Hoffmann et al. 2021). Previous direct studies on *CFL1* and SAH have been limited; however, a recent study integrating transcriptomic analysis, machine learning, and single-cell sequencing identified *CFL1* as a core immune-related gene in ischemic stroke. The study identified that *CFL1* exhibits high predictive power for ischemic stroke and that its expression is also associated with the infiltration level by various immune cells(Li et al. 2025a). This finding provides preliminary evidence for the involvement of *CFL1* in cerebrovascular diseases and related immune responses.

Ferroptosis is a key pathological process in early brain injury following SAH, primarily involving increased iron load, lipid peroxidation, oxidative stress, cellular antioxidant capacity, and mitochondrial dysfunction(Gao et al. 2020; Li et al. 2021). Cofilin-1 is highly sensitive to the redox environment, and its function is co-regulated by phosphorylation, phospholipid binding, and oxidative modifications(Samstag et al. 2013). An oxidative environment can alter the interaction between cofilin-1 and actin, thereby affecting cellular functions such as migration(Klemke et al. 2008). Consequently, given the pathological environment of oxidative stress and ferroptosis following SAH, it can be inferred that *CFL1* may participate in SAH onset and progression by regulating the cytoskeleton and cell adaptation to an oxidative environment. The above studies provide a biological basis for the association between *CFL1* genetic prediction of expression and SAH risk observed in this study.

Based on this causal inference, we further identified that the regulatory role of *CFL1* in SAH was more pronounced in a class of immune cells, CD8NC. This suggests that the function of this gene may be immune cell type-specific. In the sc-eQTL data used in this study, CD8NC primarily comprised $CD8^+$ naive and central memory T cells. However, direct studies on the relationship between CD8NC and SAH are lacking. Existing evidence suggests that $CD8^+$ T cells are involved in the immune response following SAH. $CD8^+$ T cells in the cerebrospinal fluid (CSF) of patients with aneurysmal SAH exhibit high activation levels(Moraes et al. 2015), and $CD8^+CD161^+$ lymphocytes may increase in the CSF as the disease progresses, a phenomenon that is more pronounced in patients with cerebral vasospasm(Roa et al. 2020). Following SAH, CXCL12 derived from cerebral vascular endothelial cells and pericytes can promote $CD8^+$ T cell infiltration into the brain tissue via CXCR4, thereby exacerbating blood-brain barrier dysfunction(Li et al. 2025b).

Changes in the cytoskeleton of cerebral vascular endothelial cells may provide a structural basis for recruiting these immune cells. A study using proteomic and transcriptomic analyses identified that, under inflammatory conditions, cofilin-1- and Arp2/3-mediated actin remodeling is enhanced in cerebral microvascular endothelial cells, promoting the formation of membrane protrusions and clustering of cell adhesion molecules, thereby providing a structural foundation for the adhesion and transendothelial

migration of immune cells(Lichtenberg et al. 2025). Following *CFL1* knockdown in endothelial cells, the number of T cells adhering to inflammatory conditions was significantly reduced. Based on these findings, we can infer that *CFL1* may influence the peripheral immune cell recruitment to the central nervous system by regulating the morphology of cerebral vascular endothelial cells and the spatial distribution of adhesion molecules. Furthermore, cofilin-1-mediated changes in actin are crucial for T cells to form immunosynapses, complete receptor redistribution(Eibert et al. 2004), and migrate directionally within tissues(Klemke et al. 2010). T-cell receptors and co-stimulatory signals can initiate cytoskeletal remodeling by promoting cofilin-1 dephosphorylation.

Conversely, an oxidative environment may inhibit its normal function, leading to reduced T-cell migration or a hyporesponsive state(Wabnitz et al. 2006; Klemke et al. 2008). Based on this, it is hypothesized that genetic variations in *CFL1* expression in CD8NC cells may simultaneously affect the cytoskeletal remodeling and chemotactic migration capacity of this cell subset and its interactions with cerebral vascular endothelial cells, thereby contributing to SAH risk. In summary, genetic variations in *CFL1* expression in CD8NC cells may simultaneously affect cytoskeletal remodeling and chemotactic migration capabilities of this cell subset, and its interactions with cerebral vascular endothelial cells, thereby contributing to SAH risk. This hypothesis ties together three previously disparate lines of research: The immune-inflammatory response in SAH, the involvement of CD8-associated immune cells in SAH progression, and cofilin-1-mediated cytoskeletal and stress regulation. However, this study does not directly demonstrate that the *CFL1* gene influences SAH onset and progression via CD8NC cells; instead, it provides preliminary evidence for a "*CFL1* gene-CD8NC cell-specific regulatory axis" from a genetic causality perspective. This finding provides new leads for subsequent validation of the underlying mechanisms and for the exploration of cell-type-specific targets.

4.2 Study Strengths, Limitations, and Future Directions

The strength of this study is establishing an integrated framework comprising eQTLGen for initial screening, GTEx for validation, GEO transcriptomic cross-validation, and sc-eQTL analysis. eQTLGen provides large-scale genetic regulation data for gene expression in blood, GTEx provides tissue-specific genetic regulation resources, and sc-eQTL data further enhance cell-type resolution. MR analysis uses genetic variation as an instrumental variable, helping reduce the impact of confounding factors and reverse-causation bias in traditional observational studies. This study adheres to STROBE-MR reporting guidelines and assesses the robustness of results through heterogeneity, polypleiotropy, and sensitivity analyses, thereby enhancing the credibility of findings.

This study has certain limitations. First, GWAS, eQTL, and sc-eQTL data used in this study were primarily derived from European populations; therefore, the applicability of results to other ethnic groups requires further validation. Second, although sc-eQTLs can improve cell-type resolution, they are essentially based on genetic statistical inference and cannot directly reflect the dynamic functional state of CD8NC cells following SAH. Furthermore, given the limited number of available instrumental variables in some sc-eQTL analyses, cell-type-specific results should still be considered exploratory findings.

Future studies could further integrate single-cell transcriptomic, spatial transcriptomic, proteomic, and immunological assays in patients with SAH to validate the specific regulatory role of the *CFL1* gene in CD8 + cells. Animal models and cellular experiments could further clarify whether the *CFL1* gene contributes to secondary brain injury following SAH by influencing CD8 + immune cell infiltration, blood-brain barrier damage, oxidative stress responses, or ferroptosis-related pathways. Large-scale prospective studies and randomized controlled trials are required to further validate the clinical value of the *CFL1* gene and related ferroptosis pathways in SAH and to advance their clinical translation into precision interventions and targeted treatment strategies.

5 Conclusions

Based on a dual eQTL database, GEO expression validation, and sc-eQTL data, this study identified a relatively stable genetic association between upregulation of the ferroptosis-related gene *CFL1* and a reduced risk of SAH. Moreover, this study observed that the genetic regulatory effects of *CFL1* exhibit a degree of cell-type specificity in CD8NC cells. These findings provide genetic clues for further elucidating the mechanisms underlying the interaction between ferroptosis-related genes and immune cells in SAH and provide potential avenues for subsequent mechanistic validation and target identification.

Abbreviations

eQTL
expression quantitative trait locus
GEO
Gene Expression Omnibus
GTEx
Genotype-Tissue Expression
GWAS
genome-wide association study
IV
instrumental variable
IVW
inverse-variance weighted
LD
linkage disequilibrium
MR
Mendelian randomization
MR-PRESSO
Mendelian Randomization Pleiotropy RESidual Sum and Outlier
NK
natural killer
n**SNP**

number of single-nucleotide polymorphisms
OR
odds ratio
ROS
reactive oxygen species
SAH
subarachnoid hemorrhage
sc-eQTL
single-cell expression quantitative trait locus
SE
standard error
SLC7A11
solute carrier family 7 member 11
SNP
single-nucleotide polymorphism
STROBE-MR
Strengthening the Reporting of Observational Studies in Epidemiology using Mendelian Randomization
WM
weighted median
WR
Wald ratio.

Declarations

Competing Interests

The authors declare that they have no competing interests.

Ethics Approval and Consent to Participate

This study used publicly available summary-level or de-identified data from previously approved studies and involved no new participant recruitment or primary data collection. Ethical approval and informed consent were obtained by the original studies as applicable; therefore, no additional ethics approval or consent to participate was required for this secondary analysis.

Funding

This work was supported by the Taishan Scholar Project (tsqn202312392); the youth talent training program from Qingdao medical college of Qingdao University (RZ2300002690).

Author Contribution

Xiaohan Yang: Writing – original draft, Writing – review & editing, Visualization, Validation, Resources, Methodology, Investigation, Data curation. Dantong Han: Writing – original draft, Writing – review & editing, Visualization, Validation, Resources, Methodology, Investigation, Data curation. Shaowan Yang: Writing – original draft, Writing – review & editing, Visualization, Validation, Resources, Methodology, Investigation, Data curation. Han Meng: Validation, Resources, Methodology. Xiaodi Chen: Validation, Methodology, Investigation, Data curation. Xiao Xiao: Writing – review & editing, Project administration, Formal analysis, Conceptualization. Jiajia Yun: Writing – review & editing, Supervision, Project administration, Formal analysis, Conceptualization. Chao Ren: Writing – review & editing, Supervision, Project administration, Funding acquisition, Formal analysis, Conceptualization,Guarantor.

Acknowledgments

We would like to thank the eQTLGen Consortium, the Genotype-Tissue Expression (GTEx) project, the FerrDb database, the Gene Expression Omnibus (GEO) database, the FinnGen project (release R12), and the research teams behind the single-cell eQTL data resources for providing publicly available genomic data resources for this study. We would like to thank Researchers' Home for providing technical support regarding the use of relevant plotting software. The data sharing and technical support mentioned above were instrumental in the successful completion of this study, we sincerely thank the editorial team at Home for Researchers (www.home-for-researchers.com) for their language editing services. The authors reviewed and edited the content as needed and take full responsibility for the final publication.

Data Availability

All data analyzed in this study were obtained from publicly available databases and previously published studies. Ferroptosis-related gene data were obtained from the FerrDb database. Whole-blood expression quantitative trait locus (eQTL) data were obtained from the eQTLGen Consortium and the Genotype-Tissue Expression (GTEx) Project, with GTEx Whole_Blood.v10.eQTLs used for independent validation. The single-cell eQTL (sc-eQTL) data across 14 immune cell types were derived from the study by Yazar et al. The summary-level genome-wide association study data for subarachnoid hemorrhage were obtained from FinnGen Consortium Release 12, using the phenotype I9_SAH. Transcriptomic data used for differential expression validation were obtained from the Gene Expression Omnibus under accession number GSE13353 (platform GPL570). All data used in the present study are publicly available from the corresponding original studies, databases, and consortia. Additional data generated during the analyses are provided in the main text and Supplementary Materials.

References

1. The GTEx Consortium (2020) The GTEx Consortium atlas of genetic regulatory effects across human tissues. Science 369:1318–1330. https://doi.org/10.1126/science.aaz1776
2. Boehm FJ, Zhou X (2022) Statistical methods for Mendelian randomization in genome-wide association studies: A review. Comput Struct Biotechnol J 20:2338–2351. https://doi.org/10.1016/j.csbj.2022.05.015
3. Bowden J, Davey Smith G, Burgess S (2015) Mendelian randomization with invalid instruments: effect estimation and bias detection through Egger regression. Int J Epidemiol 44:512–525. https://doi.org/10.1093/ije/dyv080
4. Bowden J, Davey Smith G, Haycock PC, Burgess S (2016) Consistent Estimation in Mendelian Randomization with Some Invalid Instruments Using a Weighted Median Estimator. Genet Epidemiol 40:304–314. https://doi.org/10.1002/gepi.21965
5. Bowden J, Del Greco MF, Minelli C, Davey Smith G, Sheehan N, Thompson J (2017) A framework for the investigation of pleiotropy in two-sample summary data Mendelian randomization. Stat Med 36:1783–1802. https://doi.org/10.1002/sim.7221
6. Burgess S, Thompson SG (2011) Bias in causal estimates from Mendelian randomization studies with weak instruments. Stat Med 30:1312–1323. https://doi.org/10.1002/sim.4197
7. Burgess S, Butterworth A, Thompson SG (2013) Mendelian randomization analysis with multiple genetic variants using summarized data. Genet Epidemiol 37:658–665. https://doi.org/10.1002/gepi.21758
8. Burgess S, Davey Smith G, Davies NM, Dudbridge F, Gill D, Glymour MM, Hartwig FP, Kutalik Z, Holmes MV, Minelli C, Morrison JV, Pan W, Relton CL, Theodoratou E (2019) Guidelines for performing Mendelian randomization investigations: update for summer 2023. Wellcome Open Res 4:186. https://doi.org/10.12688/wellcomeopenres.15555.3
9. Davies NM, Holmes MV, Davey Smith G (2018) Reading Mendelian randomisation studies: a guide, glossary, and checklist for clinicians. BMJ 362:k601. https://doi.org/10.1136/bmj.k601
10. Deng X, Wu Y, Hu Z, Wang S, Zhou S, Zhou C, Gao X, Huang Y (2023) The mechanism of ferroptosis in early brain injury after subarachnoid hemorrhage. Front Immunol 14:1191826. https://doi.org/10.3389/fimmu.2023.1191826
11. Dixon SJ, Lemberg KM, Lamprecht MR, Skouta R, Zaitsev EM, Gleason CE, Patel DN, Bauer AJ, Cantley AM, Yang WS, Morrison B 3rd, Stockwell BR (2012) Ferroptosis: an iron-dependent form of nonapoptotic cell death. Cell 149:1060–1072. https://doi.org/10.1016/j.cell.2012.03.042
12. Duan M, Xu Y, Li Y, Feng H, Chen Y (2024) Targeting brain-peripheral immune responses for secondary brain injury after ischemic and hemorrhagic stroke. J Neuroinflammation 21:102. https://doi.org/10.1186/s12974-024-03101-y
13. Eibert SM, Lee KH, Pipkorn R, Sester U, Wabnitz GH, Giese T, Meuer SC, Samstag Y (2004) Cofilin peptide homologs interfere with immunological synapse formation and T cell activation. Proc Natl Acad Sci U S A 101:1957–1962. https://doi.org/10.1073/pnas.0308282100

14. Etminan N, Macdonald RL (2017) Management of aneurysmal subarachnoid hemorrhage. Handb Clin Neurol 140:195–228. https://doi.org/10.1016/b978-0-444-63600-3.00012-x
15. Gao SQ, Liu JQ, Han YL, Deji QZ, Zhaba WD, Deng HJ, Liu XL, Zhou ML (2020) Neuroprotective role of glutathione peroxidase 4 in experimental subarachnoid hemorrhage models. Life Sci 257:118050. https://doi.org/10.1016/j.lfs.2020.118050
16. Grover S, Del Greco MF, Stein CM, Ziegler A (2017) Mendelian Randomization. Methods Mol Biol 1666:581–628. https://doi.org/10.1007/978-1-4939-7274-6_29
17. Hartley AE, Power GM, Sanderson E, Smith GD (2022) A Guide for Understanding and Designing Mendelian Randomization Studies in the Musculoskeletal Field. JBMR Plus 6:e10675. https://doi.org/10.1002/jbm4.10675
18. Hartwig FP, Davey Smith G, Bowden J (2017) Robust inference in summary data Mendelian randomization via the zero modal pleiotropy assumption. Int J Epidemiol 46:1985–1998. https://doi.org/10.1093/ije/dyx102
19. Hayden SM, Miller PS, Brauweiler A, Bamburg JR (1993) Analysis of the interactions of actin depolymerizing factor with G- and F-actin. Biochemistry 32:9994–10004. https://doi.org/10.1021/bi00089a015
20. Hemani G, Tilling K, Davey Smith G (2017) Orienting the causal relationship between imprecisely measured traits using GWAS summary data. PLoS Genet 13:e1007081. https://doi.org/10.1371/journal.pgen.1007081
21. Hoffmann L, Waclawczyk MS, Tang S, Hanschmann EM, Gellert M, Rust MB, Culmsee C (2021) Cofilin1 oxidation links oxidative distress to mitochondrial demise and neuronal cell death. Cell Death Dis 12:953. https://doi.org/10.1038/s41419-021-04242-1
22. Hoh BL et al (2023) 2023 Guideline for the Management of Patients With Aneurysmal Subarachnoid Hemorrhage: A Guideline From the American Heart Association/American Stroke Association. Stroke 54:e314–e370. https://doi.org/10.1161/str.0000000000000436
23. Hu X, Cai M, Xiao J, Wan X, Wang Z, Zhao H, Yang C (2024) Benchmarking Mendelian randomization methods for causal inference using genome-wide association study summary statistics. Am J Hum Genet 111:1717–1735. https://doi.org/10.1016/j.ajhg.2024.06.016
24. Jin J, Hu J, Li M, Gu W, Jiang X, Stockwell BR (2026) Ferroptosis as an approach to leverage cancer metabolism. Trends Cell Biol 36:545–560. https://doi.org/10.1016/j.tcb.2026.03.008
25. Kang J, Tian S, Zhang L, Yang G (2024) Ferroptosis in early brain injury after subarachnoid hemorrhage: review of literature. Chin Neurosurg J 10:6. https://doi.org/10.1186/s41016-024-00357-4
26. Klemke M, Kramer E, Konstandin MH, Wabnitz GH, Samstag Y (2010) An MEK-cofilin signalling module controls migration of human T cells in 3D but not 2D environments. Embo j 29:2915–2929. https://doi.org/10.1038/emboj.2010.153
27. Klemke M, Wabnitz GH, Funke F, Funk B, Kirchgessner H, Samstag Y (2008) Oxidation of cofilin mediates T cell hyporesponsiveness under oxidative stress conditions. Immunity 29:404–413.

https://doi.org/10.1016/j.immuni.2008.06.016

28. Kuang H, Wang T, Liu L, Tang C, Li T, Liu M, Wang T, Zhong W, Wang Y (2021) Treatment of early brain injury after subarachnoid hemorrhage in the rat model by inhibiting p53-induced ferroptosis. Neurosci Lett 762:136134. https://doi.org/10.1016/j.neulet.2021.136134
29. Kurki MI et al (2023) FinnGen provides genetic insights from a well-phenotyped isolated population. Nature 613:508–518. https://doi.org/10.1038/s41586-022-05473-8
30. Li T, Kang X, Zhang S, Wang Y, He J, Li H, Shao C, Kang J (2025a) Integrating machine learning and multi-omics analysis to reveal nucleotide metabolism-related immune genes and their functional validation in ischemic stroke. Front Immunol 16:1561544. https://doi.org/10.3389/fimmu.2025.1561544
31. Li X, Zeng L, Lu X, Chen K, Yu M, Wang B, Zhao M (2023) Early Brain Injury and Neuroprotective Treatment after Aneurysmal Subarachnoid Hemorrhage: A Literature Review. Brain Sci 13. https://doi.org/10.3390/brainsci13071083
32. Li Y, Liu Y, Wu P, Tian Y, Liu B, Wang J, Bihl J, Shi H (2021) Inhibition of Ferroptosis Alleviates Early Brain Injury After Subarachnoid Hemorrhage In Vitro and In Vivo via Reduction of Lipid Peroxidation. Cell Mol Neurobiol 41:263–278. https://doi.org/10.1007/s10571-020-00850-1
33. Li Y, Ru X, Xu Y, Guo P, Zhou J, Li W, Duan M, Kang W, Lin J, Zhang X, Li W, Chen Z, Feng H, Chen Y (2025b) Single-cell sequencing reveals intracranial microvasculature-derived CXCL12 promotes CD8(+) T-cell infiltration and blood-brain barrier dysfunction after subarachnoid hemorrhage in mice. J Neuroinflammation 22:116. https://doi.org/10.1186/s12974-025-03444-0
34. Lichtenberg S et al (2025) The potassium channel K(2P)2.1 shapes the morphology and function of brain endothelial cells via actin network remodeling. Nat Commun 16:6622. https://doi.org/10.1038/s41467-025-61816-9
35. Liu Z, Zhou Z, Ai P, Zhang C, Chen J, Wang Y (2022) Astragaloside IV attenuates ferroptosis after subarachnoid hemorrhage via Nrf2/HO-1 signaling pathway. Front Pharmacol 13:924826. https://doi.org/10.3389/fphar.2022.924826
36. Ma X, Xiao L, Liu L, Ye L, Su P, Bi E, Wang Q, Yang M, Qian J, Yi Q (2021) CD36-mediated ferroptosis dampens intratumoral CD8(+) T cell effector function and impairs their antitumor ability. Cell Metab 33:1001–1012e1005. https://doi.org/10.1016/j.cmet.2021.02.015
37. Moraes L, Grille S, Morelli P, Mila R, Trias N, Brugnini A, N LL, Biestro A, Lens D (2015) Immune cells subpopulations in cerebrospinal fluid and peripheral blood of patients with Aneurysmal Subarachnoid Hemorrhage. Springerplus 4:195. https://doi.org/10.1186/s40064-015-0970-2
38. Pavlides JM, Zhu Z, Gratten J, McRae AF, Wray NR, Yang J (2016) Predicting gene targets from integrative analyses of summary data from GWAS and eQTL studies for 28 human complex traits. Genome Med 8:84. https://doi.org/10.1186/s13073-016-0338-4
39. Paz V, Dashti HS, Burgess S, Garfield V (2023) Selection of genetic instruments in Mendelian randomisation studies of sleep traits. Sleep Med 112:342–351. https://doi.org/10.1016/j.sleep.2023.10.036

40. Pfnür A, Mayer B, Dörfer L, Tumani H, Spitzer D, Huber-Lang M, Kapapa T (2025) Regulatory T Cell- and Natural Killer Cell-Mediated Inflammation, Cerebral Vasospasm, and Delayed Cerebral Ischemia in Aneurysmal Subarachnoid Hemorrhage-A Systematic Review and Meta-Analysis Approach. Int J Mol Sci 26. https://doi.org/10.3390/ijms26031276
41. Roa JA, Sarkar D, Zanaty M, Ishii D, Lu Y, Karandikar NJ, Hasan DM, Ortega SB, Samaniego EA (2020) Preliminary results in the analysis of the immune response after aneurysmal subarachnoid hemorrhage. Sci Rep 10:11809. https://doi.org/10.1038/s41598-020-68861-y
42. Samstag Y, John I, Wabnitz GH (2013) Cofilin: a redox sensitive mediator of actin dynamics during T-cell activation and migration. Immunol Rev 256:30–47. https://doi.org/10.1111/imr.12115
43. Shen H, Yan X, Zhao M, Sun J, Huang Y (2026) Subarachnoid hemorrhage: epidemiology, risk factors, pathogenesis, and clinical therapies. Mol Biomed 7. https://doi.org/10.1186/s43556-026-00455-y
44. Shi L, Liu Y, Li M, Luo Z (2022) Emerging roles of ferroptosis in the tumor immune landscape: from danger signals to anti-tumor immunity. Febs j 289:3655–3665. https://doi.org/10.1111/febs.16034
45. Skrivankova VW, Richmond RC, Woolf BAR, Yarmolinsky J, Davies NM, Swanson SA, VanderWeele TJ, Higgins JPT, Timpson NJ, Dimou N, Langenberg C, Golub RM, Loder EW, Gallo V, Tybjaerg-Hansen A, Davey Smith G, Egger M, Richards JB (2021) Strengthening the Reporting of Observational Studies in Epidemiology Using Mendelian Randomization: The STROBE-MR Statement. JAMA 326:1614–1621. https://doi.org/10.1001/jama.2021.18236
46. Verbanck M, Chen CY, Neale B, Do R (2018) Detection of widespread horizontal pleiotropy in causal relationships inferred from Mendelian randomization between complex traits and diseases. Nat Genet 50:693–698. https://doi.org/10.1038/s41588-018-0099-7
47. Võsa U et al (2021) Large-scale cis- and trans-eQTL analyses identify thousands of genetic loci and polygenic scores that regulate blood gene expression. Nat Genet 53:1300–1310. https://doi.org/10.1038/s41588-021-00913-z
48. Wabnitz GH, Nebl G, Klemke M, Schröder AJ, Samstag Y (2006) Phosphatidylinositol 3-kinase functions as a Ras effector in the signaling cascade that regulates dephosphorylation of the actin-remodeling protein cofilin after costimulation of untransformed human T lymphocytes. J Immunol 176:1668–1674. https://doi.org/10.4049/jimmunol.176.3.1668
49. Yazar S, Alquicira-Hernandez J, Wing K, Senabouth A, Gordon MG, Andersen S, Lu Q, Rowson A, Taylor TRP, Clarke L, Maccora K, Chen C, Cook AL, Ye CJ, Fairfax KA, Hewitt AW, Powell JE (2022) Single-cell eQTL mapping identifies cell type-specific genetic control of autoimmune disease. Science 376:eabf3041. https://doi.org/10.1126/science.abf3041
50. Zhang XD, Liu ZY, Wang MS, Guo YX, Wang XK, Luo K, Huang S, Li RF (2023a) Mechanisms and regulations of ferroptosis. Front Immunol 14:1269451. https://doi.org/10.3389/fimmu.2023.1269451
51. Zhang Z, Duan Z, Cui Y (2023b) CD8(+) T cells in brain injury and neurodegeneration. Front Cell Neurosci 17:1281763. https://doi.org/10.3389/fncel.2023.1281763

52. Zhou N, Bao J (2020) FerrDb: a manually curated resource for regulators and markers of ferroptosis and ferroptosis-disease associations. Database (Oxford) 2020. https://doi.org/10.1093/database/baaa021
53. Zhou N, Yuan X, Du Q, Zhang Z, Shi X, Bao J, Ning Y, Peng L (2023) FerrDb V2: update of the manually curated database of ferroptosis regulators and ferroptosis-disease associations. Nucleic Acids Res 51:D571–d582. https://doi.org/10.1093/nar/gkac935

Figures

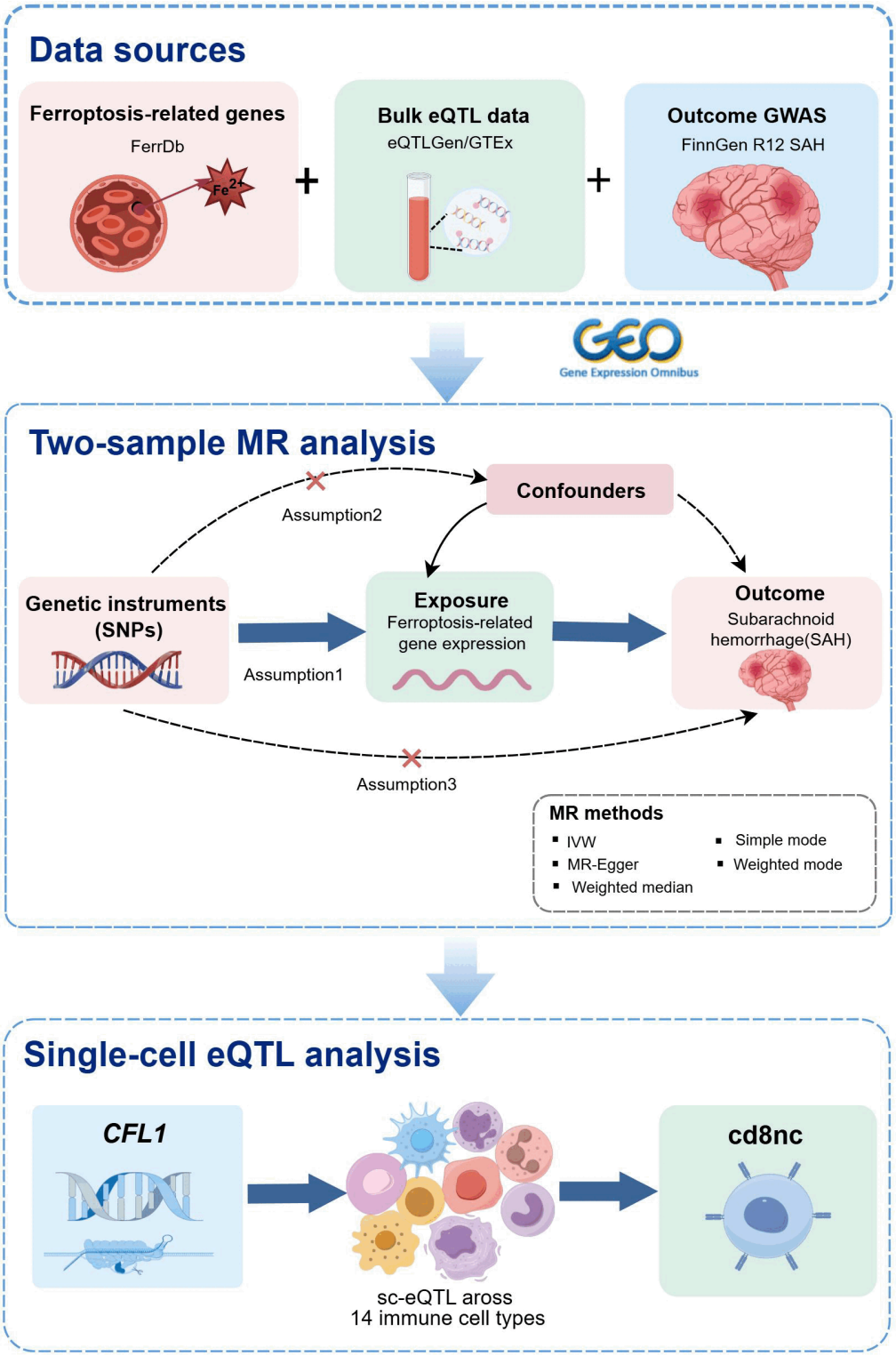


Figure 1

Flowchart of the study design and Mendelian randomization framework.

The study integrated ferroptosis-related genes, cis-eQTL summary statistics from the eQTLGen Consortium and GTEx whole blood dataset, and GWAS summary statistics for subarachnoid hemorrhage. The MR analysis was conducted under three core assumptions to ensure the validity of

genetic instrumental variables. Subsequent GEO expression validation and single-cell eQTL-based MR analysis were performed to further evaluate the potential cell-type-specific association between CFL1 expression in immune cell subtypes and subarachnoid hemorrhage.MR, Mendelian randomization; SNP, single nucleotide polymorphism; eQTL, expression quantitative trait locus; GTEx, Genotype-Tissue Expression; GEO, Gene Expression Omnibus; sceQTL, single-cell expression quantitative trait locus; SAH, subarachnoid hemorrhage; IVW, inverse variance weighted; CFL1, cofilin-1.

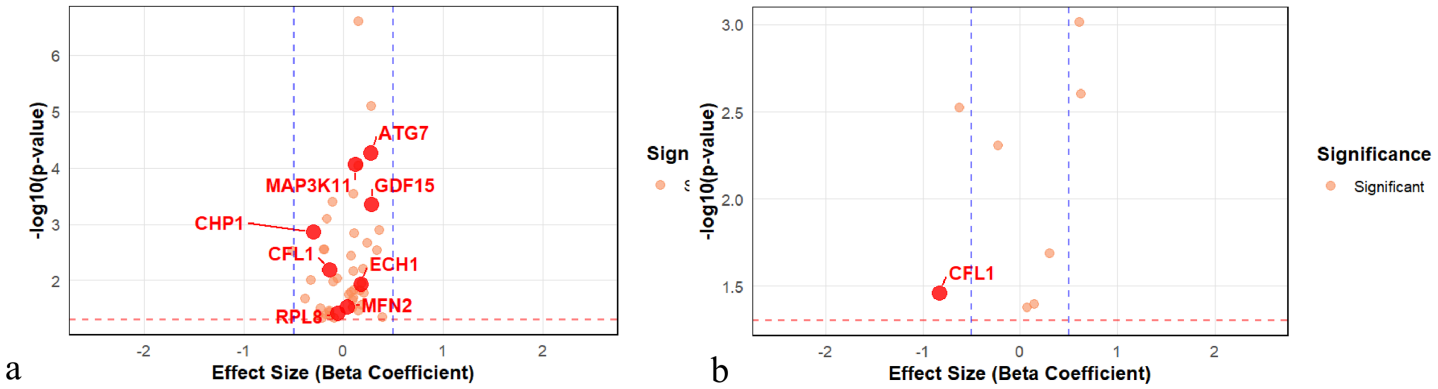


Figure 2

Volcano plots of Mendelian randomization estimates for ferroptosis-related genes associated with subarachnoid hemorrhage.

(A) Distribution of the MR effect estimates for ferroptosis-related genes based on the eQTLGen dataset. The eight genes subsequently replicated in the GTEx whole blood dataset are highlighted and labeled.

(B) Distribution of the MR effect estimates for the eight replicated genes based on the GTEx whole blood dataset. CFL1, which was further supported by GEO differential expression analysis, is highlighted. The horizontal dashed line represents the statistical significance threshold of P = 0.05. The x-axis represents the MR effect estimate (β), and the y-axis represents −log10(P value). Positive β values indicate associations with increased SAH risk, whereas negative β values indicate associations with reduced SAH risk.MR, Mendelian randomization; eQTL, expression quantitative trait locus; GTEx, Genotype-Tissue Expression; GEO, Gene Expression Omnibus; SAH, subarachnoid hemorrhage; CFL1, cofilin-1.



Figure 3

Forest plot of the causal effects of genetically predicted expression of ferroptosis-related genes on subarachnoid hemorrhage based on eQTLGen data.

OR: odds ratio; CI: confidence interval.

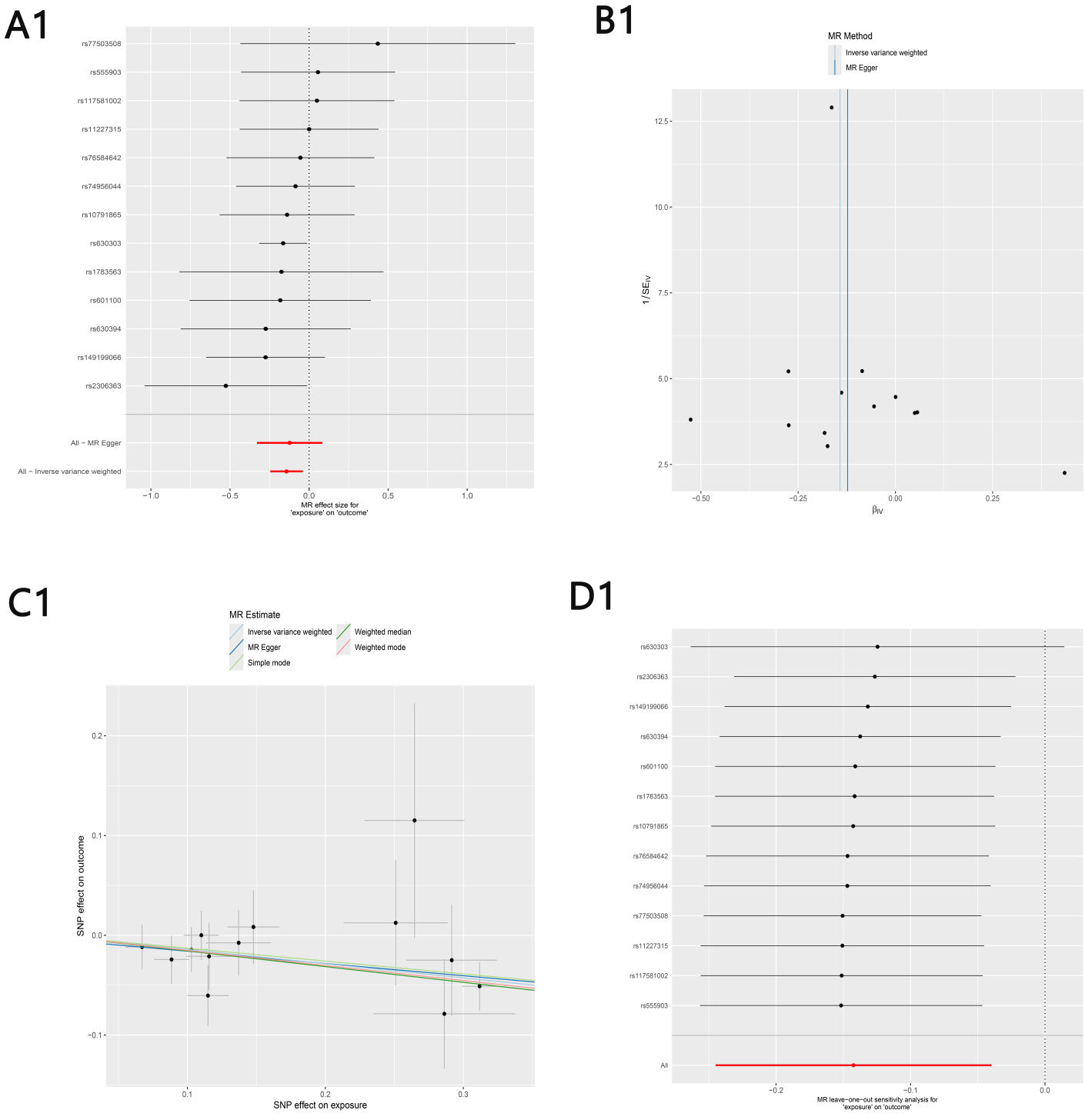


Figure 4

Sensitivity analyses for the causal effect of genetically predicted CFL1 expression on SAH.

(A1) Forest plot of individual SNP effects on SAH risk. Red lines indicate the pooled MR estimates.
(B1) Funnel plot assessing directional horizontal pleiotropy.
(C1) Scatter plot of SNP effects on CFL1 expression versus SAH.
(D1) Leave-one-out analysis evaluating the stability of the causal estimate.

SAH, subarachnoid hemorrhage; CFL1, cofilin-1; MR, Mendelian randomization; SNP, single nucleotide polymorphism; IVW, inverse variance weighted.

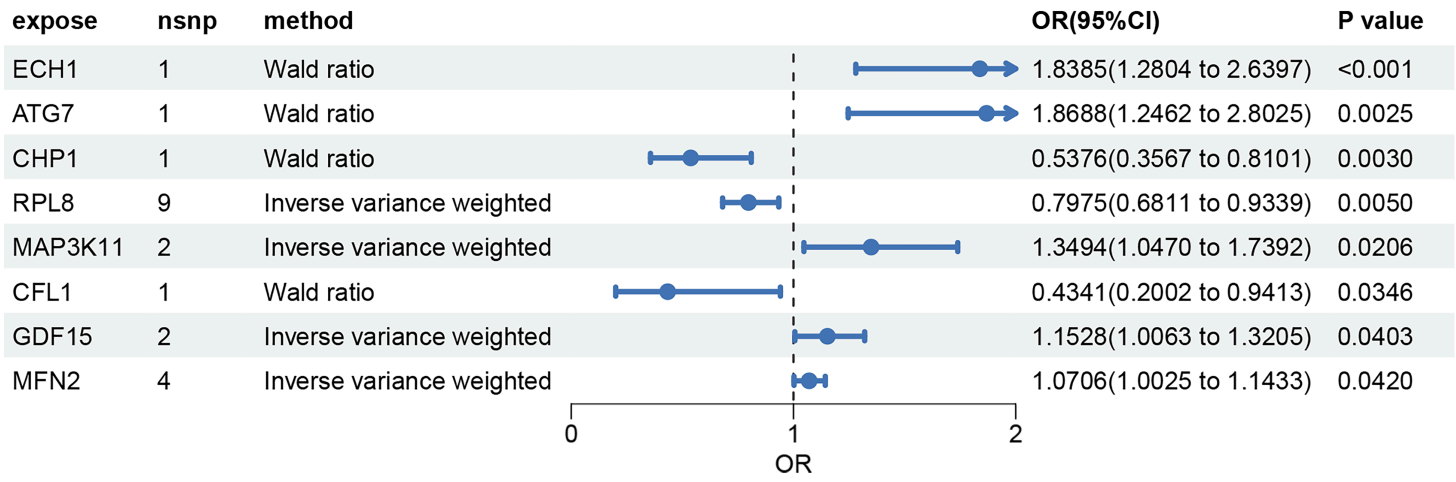


Figure 5

Validation forest plot of the causal effects of genetically predicted expression of ferroptosis-related genes on subarachnoid hemorrhage using GTEx whole blood eQTL data.

OR: odds ratio; CI: confidence interval.

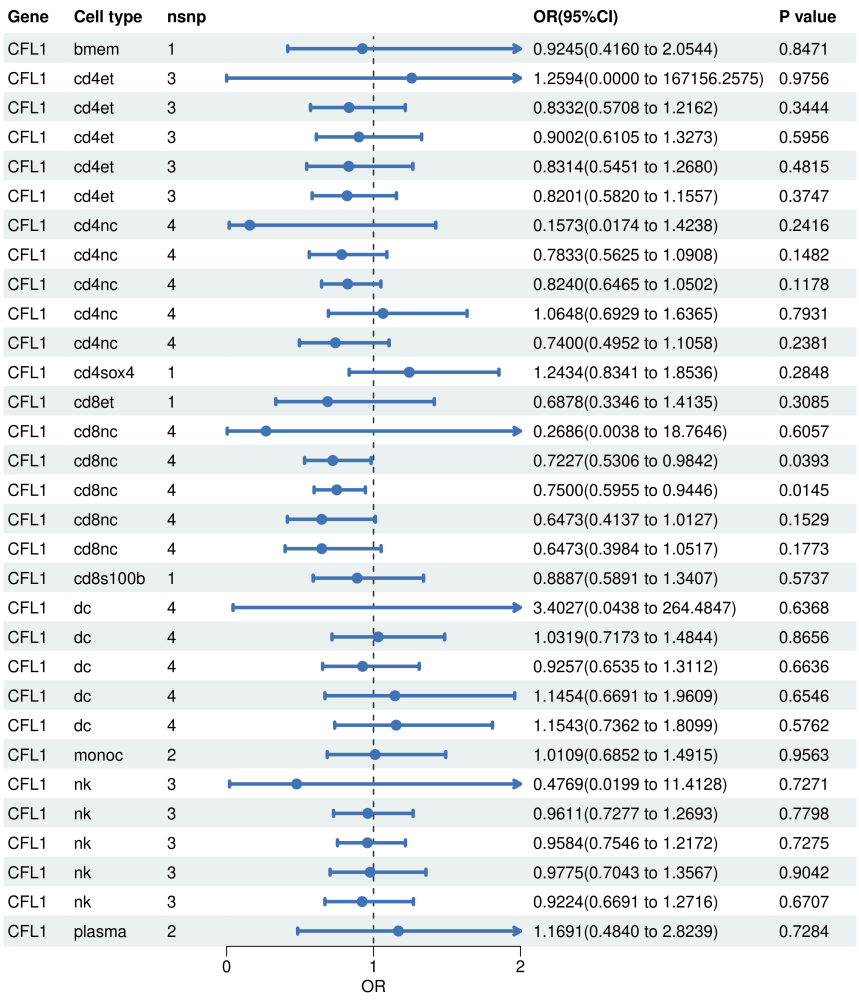


Figure 6

Forest plot of the association between genetically predicted CFL1 expression in immune cell subtypes and subarachnoid hemorrhage based on sceQTL data.

OR: odds ratio; CI: confidence interval.

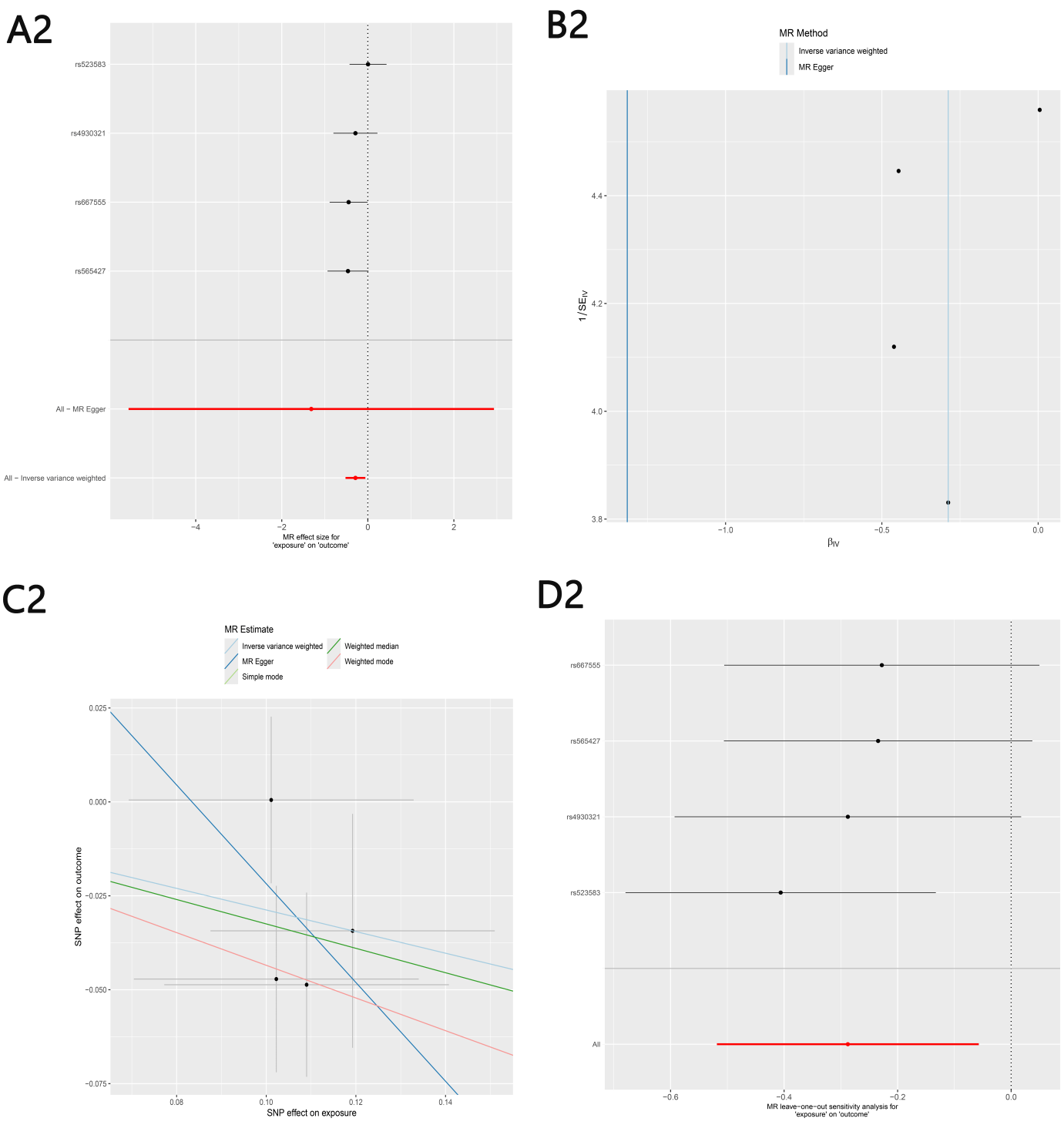


Figure 7

Sensitivity analyses for the causal effect of genetically predicted CFL1 expression in CD8NC cells on subarachnoid hemorrhage.

(A2) Forest plot of individual SNP effects on SAH risk. Red lines indicate the pooled MR estimates.
(B2) Funnel plot assessing directional horizontal pleiotropy.
(C2) Scatter plot of SNP effects on CFL1 expression in CD8NC cells versus SAH.

(D2) Leave-one-out analysis evaluating the stability of the causal estimate.
SAH, subarachnoid hemorrhage; CFL1, cofilin-1; CD8NC, CD8 natural killer-like cytotoxic cells; MR, Mendelian randomization; SNP, single nucleotide polymorphism; IVW, inverse variance weighted.

Supplementary Files

This is a list of supplementary files associated with this preprint. Click to download.

- GraphicalAbstractTitleDescription.docx
- Supplementmaterial.xlsx